ACCOUNTS
of chemical research

Electrochemical Approaches for CO_2 Conversion to Chemicals: A Journey toward Practical Applications

Published as part of the Accounts of Chemical Research special issue "CO2 Reductions via Photo and Electrochemical Processes".

Sean Overa,[†] Byung Hee Ko,[†] Yaran Zhao,[†] and Feng Jiao*

Cite This: *Acc. Chem. Res.* 2022, 55, 638−648

Read Online

ACCESS | Metrics & More | Article Recommendations

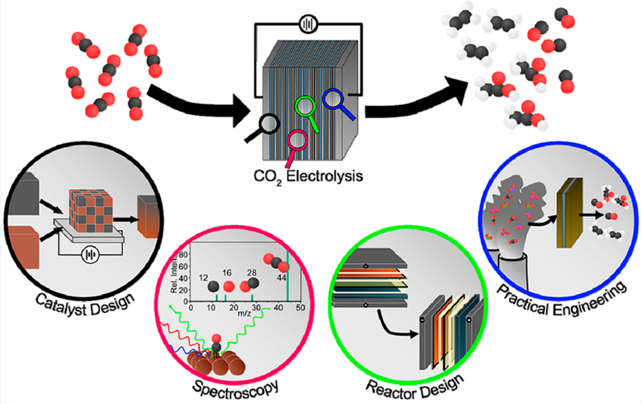

CONSPECTUS: Carbon capture, utilization, and sequestration play an essential role to address CO_2 emissions. Among all carbon utilization technologies, CO_2 electroreduction has gained immense interest due to its potential for directly converting CO_2 to a variety of valuable commodity chemicals using clean, renewable electricity as the sole energy source. The research community has witnessed rapid advances in CO_2 electrolysis technology in recent years, including highly selective catalysts, larger-scale reactors, specific process modeling, as well as a mechanistic understanding of the CO_2 reduction reaction. The rapid advances in the field brings promise to the commercial application of the technology and the rapid rollout of the CO_2 electroreduction for chemical manufacturing.

This Account focuses on our contributions in both fundamental and applied research in the field of electrocatalytic CO_2 and CO reduction reactions. We first discuss (1) the development of novel electrocatalysts for CO_2/CO electroreduction to enhance the product selectivity and lower the energy consumption. Specifically, we synthesized nanoporous Ag and homogeneously mixed Cu-based bimetallic catalysts for the enhanced production of CO from CO_2 and multicarbon products from CO, respectively. Then, we review our efforts in (2) the field of reactor engineering, including a dissolved CO_2 H-type cell, vapor-fed CO_2 three-compartment flow cell, and vapor-fed CO_2 membrane electrode assembly, for enhancing reaction rates and scalability. Next, we describe (3) the investigation of reaction mechanisms using in situ and operando techniques, such as surface-enhanced vibrational spectroscopies and electrochemical mass spectroscopy. We revealed the participation of bicarbonate in CO_2 electroreduction on Au using attenuated total-reflectance surface-enhanced infrared absorption spectroscopy, the presence of an "oxygenated" surface of Cu under CO electroreduction conditions using surface-enhanced Raman spectroscopy, and the origin of oxygen in acetaldehyde and other CO electroreduction products on Cu using flow electrolyzer mass spectrometry. Lastly, we examine (4) the commercial potential of the CO_2 electrolysis technology, such as understanding pollutant effects in CO_2 electroreduction and developing techno-economic analysis. Specifically, we discuss the effects of SO_2 and NO_x in CO_2 electroreduction using Cu, Ag, and Sn catalysts. We also identify technical barriers that need to be overcome and offer our perspective on accelerating the commercial deployment of the CO_2 electrolysis technology.

KEY REFERENCES

- Jouny, M.; Luc, W.; Jiao, F. High-rate electroreduction of carbon monoxide to multicarbon products *Nat. Catal.* **2018**, *1*, 748−755[1] *By incorporating a copper electrocatalyst into a microfluidic reactor, the reaction rate of CO electroreduction was enhanced for nearly 3 orders of magnitude, reaching an industry-relevant current density of 800 mA/cm^2.*
- Luc, W.; Ko, B. H.; Kattel, S.; Li, S.; Su, D.; Chen, J. G.; Jiao, F.; SO_2-Induced Selectivity Change in CO_2 Electroreduction *J. Am. Chem. Soc.* **2019**, *141*, 9902−9909[2] *The influence of SO_2, a common contaminant in flue gases, in CO_2 electroreduction was investigated. Copper*

Received: October 28, 2021
Published: January 18, 2022

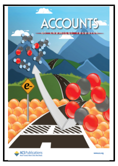

https://doi.org/10.1021/acs.accounts.1c00674

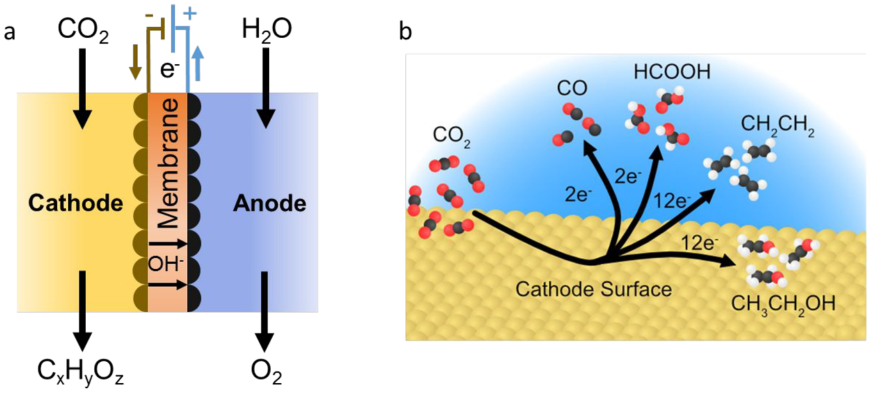

c

Species	Cathodic Half Reaction	Catalysts
Carbon Monoxide	$CO_2 + 2e^- + H_2O \rightarrow CO + 2OH^-$	Ag, Au, Pd, Zn
Formic Acid	$CO_2 + 2e^- + 2H_2O \rightarrow HCOOH + 2OH^-$	Sn, Pb, Bi, In
Ethylene	$2CO_2 + 12e^- + 8H_2O \rightarrow CH_2CH_2 + 12OH^-$	Cu
Ethanol	$2CO_2 + 12e^- + 9H_2O \rightarrow CH_3CH_2OH + 12OH^-$	Cu
Species	**Anodic Half Reaction**	
Oxygen	$4OH^- \rightarrow O_2 + 4e^- + 2H_2O$	Ir, $NiFeO_x$

Figure 1. CO_2 electroreduction reactions and products. (a) Schematic of a typical CO_2 electrolyzer. The cathode chamber utilizes electrons to reduce CO_2 to a variety of carbon-containing products. An anion-exchange membrane is used to separate the cathode and anode. (b) Schematic of the CO_2 electroreduction cathode surface. CO_2 is reduced to a variety of products, including carbon monoxide (CO), formic acid (HCOOH), ethylene (CH_2CH_2), and ethanol (CH_2CH_2OH) at the cathode surface. (c) Half-cell reactions for CO_2 electroreduction in alkaline aqueous conditions. Anodic half-cell reaction is the oxygen evolution reaction. Typical electrocatalysts used for each reaction are listed.

catalysts exhibited a high sensitivity to the presence of SO_2 even at an extremely low concentration.

- Zhao, Y.; Chang, X.; Malkani, A. S.; Yang, X.; Thompson, L.; Jiao, F.; Xu, B.; Speciation of Cu Surfaces during the Electrochemical CO Reduction Reaction *J. Am. Chem. Soc.* **2020**, *142*, 9735−9743[3] *Surface speciation of the various copper surfaces was investigated under alkaline CO electroreduction conditions via surface-enhanced Raman spectroscopy, revealing that the oxygen-containing species on the copper surface do not assist the formation of multicarbon oxygenates.*
- Shin, H.; Kentaro, H.; Jiao, F. Techno-economic assessment of low-temperature carbon dioxide electrolysis *Nat. Sustain.* **2021**, *4*, 911−919[4] *The economic aspects of low-temperature CO_2 electroreduction technology were investigated to identify the critical technical gaps, which provide guidelines for future research and market deployment.*

1. INTRODUCTION

There is an urgent need to reduce carbon dioxide (CO_2) emissions due to the imminent threat of climate change.[5] Significant effort has been devoted to developing advanced technologies for carbon capture, utilization, and storage (CCUS) to mitigate CO_2 emissions.[6] As renewable electricity becomes abundant and affordable, CO_2 conversion to value-added chemicals through electrochemical methods attracts much attention.[7] Typical CO_2 electrolyzers reduce CO_2 to hydrocarbons and oxygenates at the cathode, whereas water is oxidized to oxygen at the anode (Figure 1a). In most ambient condition reactors, the cathode and anode chambers are physically separated by an ion-conducting polymer membrane, which readily conducts charged ions but blocks the crossover of redox-active species.[8,9] Currently, a number of chemicals can be produced with appreciable selectivity, including single-carbon (C_1) products, such as formate and carbon monoxide (CO), and multicarbon (C_{2+}) products such as ethanol, ethylene, and *n*-propanol (Figure 1b).[10−26] The typical half-reactions involved in CO_2 electrolyzers and their associated electrocatalysts are summarized in Figure 1c.

Over the past decade, significant progress has been made to advance the CO_2 electrolysis technology, making it promising for commercialization.[20,21,23,27,28] For practical applications, the CO_2 electrolyzer must be operated under the following conditions: high current densities—fast reaction rates enable one to produce large quantities of products with a limited electrode size, maximizing the utilization of the capital investments; high Faradaic efficiencies—increased product selectivity not only improves the feedstock utilization but also reduces the downstream separation costs; high energetic efficiencies—a low applied full cell potential minimizes the energy consumption and, thus, the operation cost; high single-pass conversions—a commonly ignored parameter that determines the cost associated with the feedstock/product separation and recovery; high product concentrations—another important parameter controls the separation cost; high long-term stabilities—a robust system that can be operated for thousands of hours is required for practical applications but is rarely achieved in the CO_2 electroreduction research.

The primary question is how can a high-performance CO_2 electrolyzer that simultaneously possesses all desired properties be constructed? A highly efficient electrocatalyst for CO_2 reduction is the most critical component in enhancing the operating current density and product Faradaic and energetic

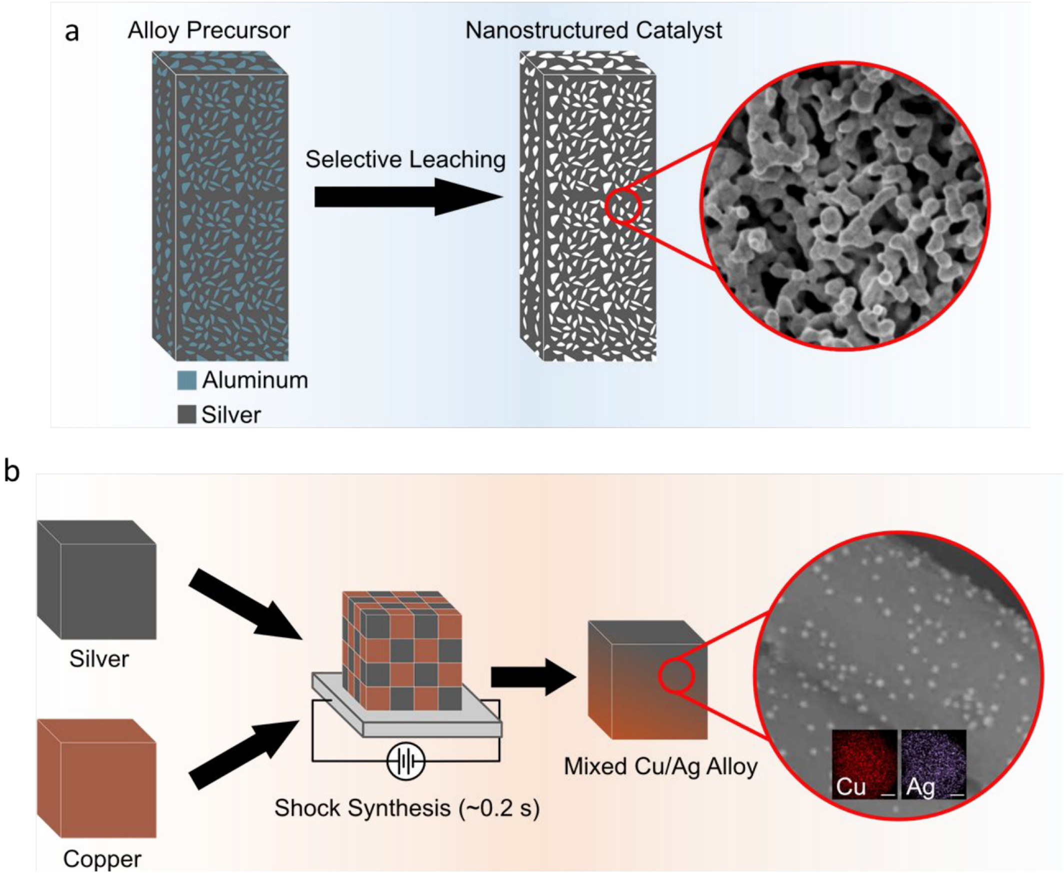

Figure 2. Investigative routes for novel catalyst designs for CO_2/CO electroreduction. Two significant routes for enhanced performance of CO_2/CO electroreduction. Routes presented include (a) nanostructuring (top left) and (b) bimetallics. Image reproduced with permission from ref 42. Copyright 2021 AAAS.

efficiencies.[10,13−18,26,29−34] Ideally, electrocatalysts possessing active sites with a high turnover frequency and suitable binding energy will promote the formation of desired products at fast rates and low overpotentials.[35] Consequently, most of the research efforts in CO_2 electroreduction have been devoted to hunting for better electrocatalysts.[36] Because of the complex nature of electrochemical systems, a high-performance CO_2 reduction electrocatalyst alone is not sufficient to meet all the requirements mentioned above for commercialization. Research efforts in reactor engineering are urgently needed to improve other important characteristics, such as single-pass conversions, product concentrations, and long-term stabilities.[23,28,37,38] This Account will discuss our approach to push CO_2 electrolysis technology toward practical applications through electrocatalyst development, reactor engineering, and operando characterizations.

2. ELECTROCATALYST DESIGN AND SYNTHESIS

Nanostructured catalysts offer a unique opportunity to modify the properties of the catalyst layer. To boost the selectivity and activity of CO_2 conversion to CO, we first designed a nanoporous Ag catalyst for the electrochemical CO_2 reduction reaction (eCO_2R).[33] Previous studies show that Ag is a selective electrocatalyst for reducing CO_2 into CO in aqueous electrolytes.[39,40] Conventional polycrystalline Ag particles require a large overpotential to obtain an appreciable current density (~5 mA cm^{-2}).[33] Studies on Ag single crystals confirm that low-coordinated Ag sites on the step surfaces have higher activities than flat surfaces.[41] Therefore, a nanostructured Ag catalyst with a high density of low-coordinated surface sites would be ideal for promoting the activity of CO_2 electroreduction to CO with high selectivity (i.e., Faradaic efficiency (FE)).

We chose to synthesize a free-standing nanoporous Ag catalyst because it can be used as an electrode directly without any conductive supports, making it a suitable candidate for fundamental studies. The nanoporous Ag was fabricated via a selective dealloying method, where aluminum (Al) was etched away from a Ag−Al bimetallic precursor to form a three-dimensional interconnected porous network (Figure 2a). The resulting nanoporous Ag was then evaluated in a three-electrode H-type cell, the standard electrochemical device for fundamental investigations. As expected, the catalyst exhibited a decent CO Faradaic efficiency (~90%) together with a high activity (~3000 times higher reaction rate than the polycrystalline Ag) under moderate overpotentials (<0.50 V). Because of the low solubility of CO_2 in the aqueous electrolyte (e.g., 1 M $KHCO_3$), the reaction rate of the Ag catalyst was limited to ~35 mA cm^{-2} in the H-type cell configuration.[33] Switching to a gas-fed flow cell configuration may improve the reaction rate; however, the nanoporous Ag catalyst is fragile and hard to incorporate into a gas-diffusion electrode (GDE) for flow reactors.

As it is easier to load nanoparticles onto gas diffusion layers (i.e., carbon paper) than free-standing nanoporous catalysts, we investigated Cu-based bimetallic nanoalloys as potential

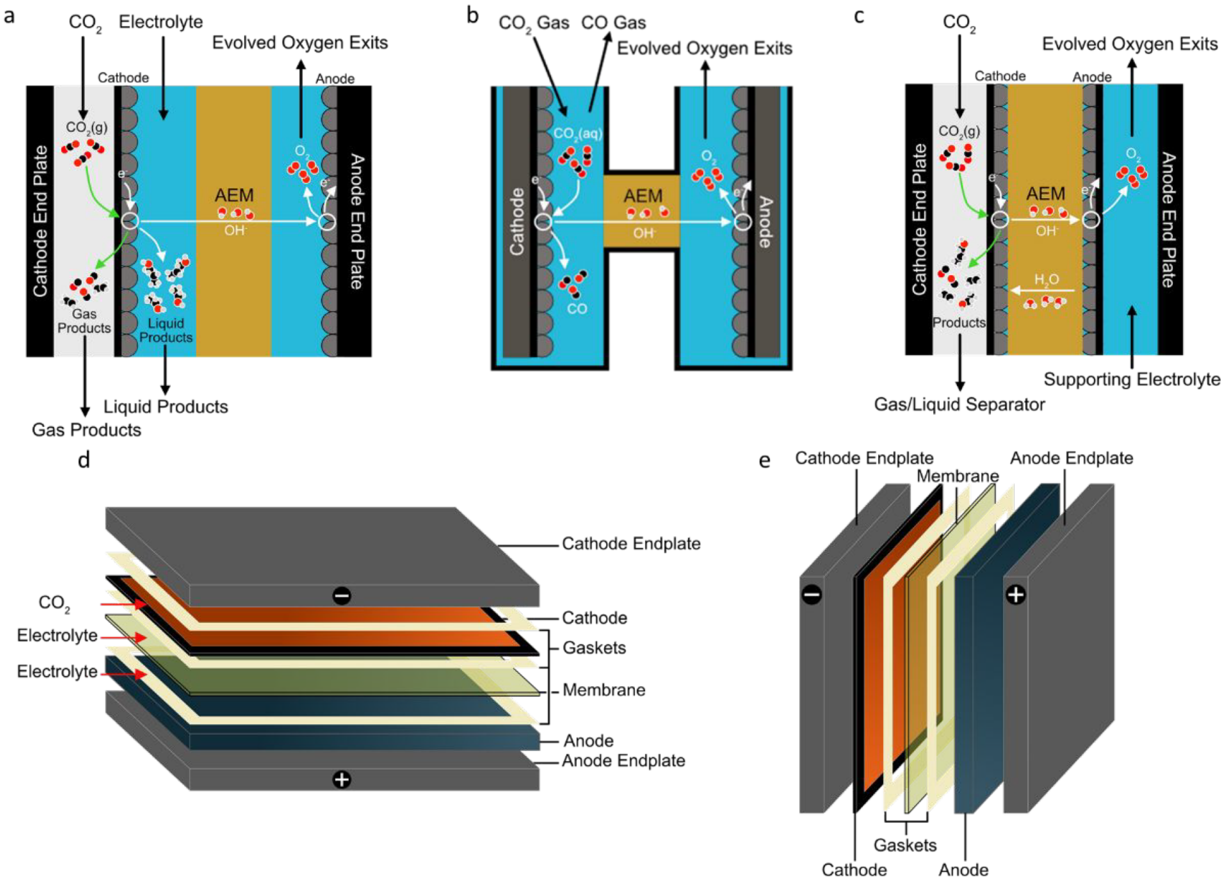

Figure 3. Schematic of common CO$_2$/CO electrolyzer configurations. (a) Three-compartment microfluidic electrolyzer, where gaseous CO$_2$ is fed to the cathode through a gas diffusion layer. Liquid electrolyte layers divide the cathode and the anode from the membrane. (b) Typical H-cell electrolyzer, where the cathode and anode are submerged in an electrolyte, gas is bubbled into the electrolyte, and the two half-cells are divided by a membrane. (c) Membrane electrode assembly electrolyzer, where gaseous CO$_2$ is fed to the cathode in direct contact with a conductive membrane and supporting electrolyte is fed to the anode also in direct contact with the membrane. Exploded views of (d) three-compartment electrolyzer and (e) membrane electrode assembly electrolyzer. Anion exchange membrane (AEM) is chosen as a membrane example. For CO electrolyzers, CO is supplied instead of CO$_2$.

catalysts for electrochemical CO reduction (eCOR).[42] Recent computational modeling has suggested that the addition of a secondary metal to the Cu would improve the energetic properties of the catalyst surface.[43,44] Therefore, the motivation behind studying these Cu-based bimetallics was to search for a combination of metals that allow for a more selective production of C$_{2+}$ products from eCOR/eCO$_2$R compared to Cu alone. In collaboration with Prof. Hu at the University of Maryland, College Park, we successfully synthesized an extensive set of homogeneously mixed Cu-based bimetallic nanocatalysts, including elements that were considered "immiscible," using a nonequilibrium high-temperature shock method (Figure 2b).[42] In conventional methods, such as galvanic replacement and seed-mediated growth, the resulting materials are greatly limited to the thermodynamically favored structures.[45−47] Consequently, it is challenging to form a large set of bimetallics with a uniform morphology but different compositions.

In contrast, by applying a thermal shock for a short time (~0.2 s), Cu and secondary metals can be kinetically trapped to obtain uniform bimetallic nanoalloys. The results showed that Cu$_{0.9}$Ag$_{0.1}$ and Cu$_{0.9}$Ni$_{0.1}$ exhibit enhanced C$_{2+}$ selectivities over pure Cu. C$_{2+}$ FE increased from 64% on Cu to 70% and 76% on Cu$_{0.9}$Ag$_{0.1}$ and Cu$_{0.9}$Ni$_{0.1}$, respectively. A small portion of Cu$_{0.9}$Ag$_{0.1}$ became phase-segregated, with Ag migrating to the surface due to the lower surface energy of Ag, whereas Cu$_{0.9}$Ni$_{0.1}$ showed no sign of phase segregation. Overall, the eCOR performance was stable, and the majority of Cu$_{0.9}$Ni$_{0.1}$ and Cu$_{0.9}$Ag$_{0.1}$ remained homogeneous under eCOR. The newly synthesized homogeneously mixed bimetallic catalysts offer access to novel materials and allow for a systematic comparison of the role of secondary metals on eCOR. Additionally, it is possible to fabricate high-entropy nanoalloys with multiple elements (up to 18 elements per particle) using a similar thermal shock method, which opens tremendous opportunities for exploring catalyst materials that cannot be accessed using conventional methods.[48] However, these high-entropy nanoalloys could be difficult for fundamental studies because of their complex nature.

3. FLOW REACTOR DESIGN

As mentioned above, flow reactors have significant advantages over dissolved CO$_2$ reactors in terms of handling gaseous reactant(s) and product(s).[49] By incorporating a gas diffusion electrode (GDE), flow reactors can overcome the mass transport issues associated with gaseous reactants, for example, CO$_2$ and CO, that are poorly soluble in aqueous electrolytes. As a result, the GDE-based flow cells can be operated at much

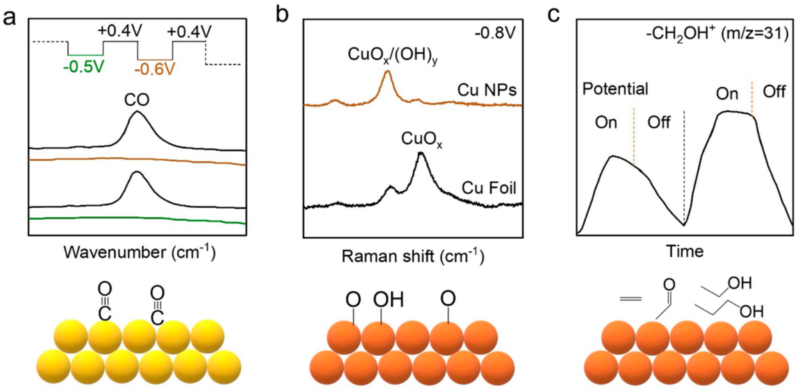

Figure 4. Spectroscopic analysis of CO_2 reduction surface. (a) ATR-SEIRAS spectra collected during square-wave electrolysis of CO_2 saturated 0.5 M $NaHCO_3$ on Au film electrodes. (b) SERS spectra of oxygenated surface species on Cu nanoparticles and foil during a CO electroreduction under −0.8 V. $CuO_x/(OH)_y$ is dominant on nanostructured Cu surfaces, whereas CuO_x is dominant on Cu foil. (c) FEMS signal of m/z = 31 during a CO electroreduction under different potentials on Cu GDE. Mass fragment $-CH_2OH^+$ is from ethanol and n-propanol products.

higher current densities (up to 1 A cm^{-2}) without compromising the product selectivity.[1] In 2017, the first-generation CO_2/CO flow electrolyzers were built in the Jiao group using an original design kindly provided by Prof. Kenis in the University of Illinois at Urbana−Champaign, known as a three-compartment microfluidic cell (Figure 3a,d).[1] In this design, eCO_2R/eCOR reduction catalyst particles are loaded onto a hydrophobic gas diffusion layer (GDL) as the cathode GDE. Then, the cathode GDE is placed between a gas chamber for the CO_2/CO feed and a liquid catholyte chamber. Using this microfluidic cell, we successfully demonstrated eCOR at a total current density of nearly 1 A cm^{-2}, which is a 3 orders of magnitude improvement over the state of the art at the time (~1 mA cm^{-2} achieved in an H-cell (Figure 3b)). This state-of-the-art performance was achieved by utilizing oxide-derived copper, an ultrahigh surface area Cu catalyst,[1,50] which allowed for greater current densities to be achieved at reduced applied potentials. Notably, the high current density was achieved with a C_{2+} FE of ~90%.

Microfluidic cells are now widely adopted by the CO_2 electrocatalysis community to evaluate electrocatalyst properties at high current densities.[19,20,51−53] While the three-compartment microfluidic cells greatly enhanced the eCO_2R/eCOR performance, the reactor design faces some challenges, such as a relatively high internal resistance due to the use of two liquid electrolyte compartments, poor stability of the electrode−electrolyte interfaces, and difficulty in scaling up to larger sizes. Suppose a 1 M KOH solution is used as the catholyte and the catholyte chamber has a thickness of 3 mm. In that case, the resistance across the catholyte layer will be 1.875 ohm cm^2, corresponding to a voltage loss of 940 mV at an operating current density of 500 mA cm^{-2}.[54] Salt accumulation and flooding are also frequently observed in the microfluidic cells during long-term operations, which cause product selectivity and cell stability issues, as the pores in the GDL are blocked.[26,55,56] Therefore, the three-compartment microfluidic cell design is an excellent choice for fundamental studies but may not be ideal for practical applications.

The internal resistance could be substantially reduced by eliminating the catholyte compartment, which converts the typical three-compartment microfluidic cell into a two-compartment flow cell. Currently, there is significant interest in developing two-compartment eCO_2R/COR cells with a membrane electrode assembly (MEA) design, as they are potentially more energetically efficient.[28,38,57,58] The MEA-based two-compartment flow reactor design (Figure 3c,e) features a GDE as the cathode, placed against an ion-conducting polymer membrane. The overall cell configuration is simpler than the microfluidic counterparts, especially when the electrolysis is conducted at elevated pressures. Recent studies show an improved energetic efficiency for the MEA-based two-compartment cells, capable of reaching higher than 100 mA cm^{-2} at less than 3 V full cell potentials.[28,57,58] The most crucial aspect of the MEA design, besides the improved energetic efficiency, is its potential in scalability. As seen with fuel cells,[59−61] the single-cell MEA design can be readily scaled into multicell stacks for commercial applications, which has been demonstrated on a small scale, where a three-cell stack was constructed to achieve 18.3 A total current density toward CO.[37]

Using the MEA-based two-compartment flow cells, we investigated the single-pass conversion of CO_2 in an electrolyzer, one of the poorly studied parameters that strongly impacts downstream product separation costs.[38] We chose Ag nanoparticles as the cathode catalyst and iridium oxide-loaded titanium support as the anode. At the optimal conditions, ~43% of CO_2 was electrochemically converted into CO in a single pass of the CO_2 feed. While this number seems low at first glance, the maximum single-pass conversion of CO_2 into CO is limited to 50% due to the bicarbonate/carbonate formation when an alkaline electrolyte (e.g., KOH) is used. Replacing the alkaline electrolyte with a neutral electrolyte (e.g., $KHCO_3$) does not solve the bicarbonate/carbonate problem because the electrode−electrolyte interface is still highly alkaline during the electrolysis, especially at high current densities. For C_{2+} products, the situation is even worse, as the maximum single-pass CO_2 conversion is limited to ~25%.[54,62] These limitations are based on the assumption that CO_3^{2-} serves as the primary charge carrier in these systems. Several alternative cell designs have been proposed to address the carbonate formation issues in the polymer membrane-based CO_2 electrolyzers, such as implementing a bipolar membrane[63−65] or a surface-coated cation exchange membrane[66] and high-temperature solid oxide electrolysis route.[67−69]

4. OPERANDO CHARACTERIZATIONS

To advance our understanding of eCO_2R and eCOR, operando characterization techniques are crucial to reveal the

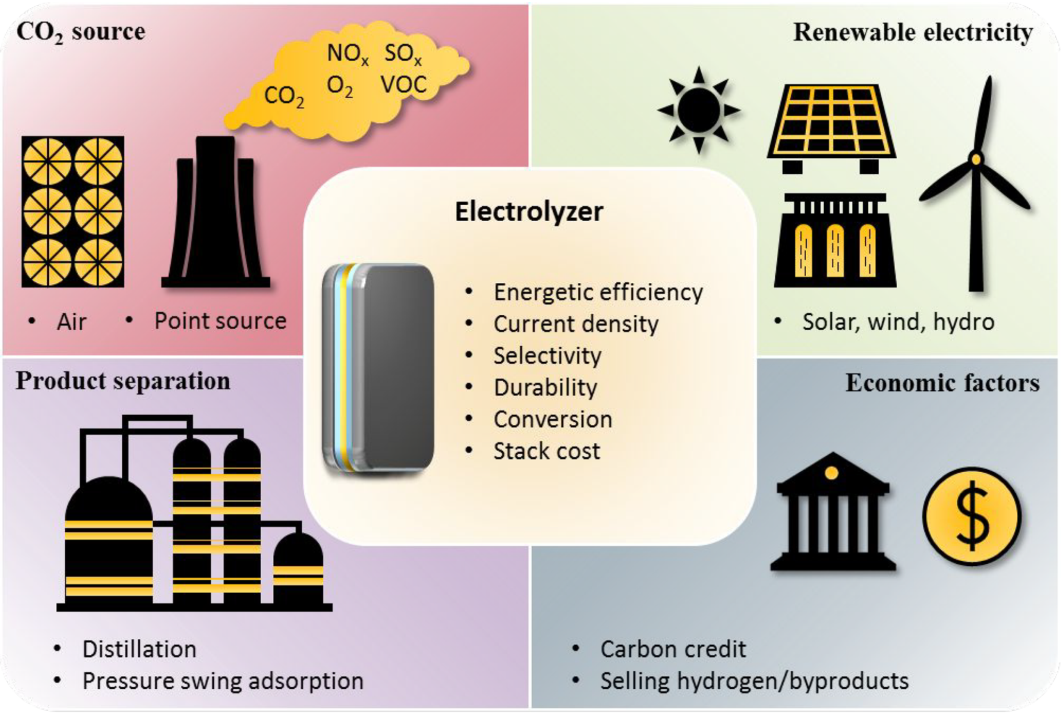

Figure 5. Consideration for practical application of CO_2 electrolysis. Critical considerations for practical CO_2 electrolysis include CO_2 sources, either from air or point sources. Renewable electricity sources such as solar, wind, and hydro. Electrolyzer performance and cost parameters. Types of product separation, such as distillation and pressure, swing absorption. Economic factors, such as carbon credit and selling hydrogen/byproducts.

reactive intermediates when the catalyst is actively catalyzing the reactions. Surface-sensitive techniques help us understand the interfacial transformation occurring on/near the electrode surface, such as the dynamics of adsorbed species and reactive intermediates.[70−72] In an early study, we used attenuated total-reflectance surface-enhanced infrared absorption spectroscopy (ATR-SEIRAS) to study a CO-selective Au catalyst in eCO_2R.[73] The ATR-SEIRAS technique selectively detects the species on/near the catalyst surface (<10 nm). While the method has a high sensitivity for detecting a C≡O triple bond vibration, CO weakly bonds to the Au surface under eCO_2R conditions. Together with Prof. Xu, we employed a square-wave potential profile, in which CO was electrocatalytically produced at negative potentials and then readsorbed at positive potentials.[74] By doing so, CO was observable using ATR-SEIRAS (Figure 4a). Using isotopic labeling methods, we successfully identified the source of CO_2 during eCO_2R in aqueous bicarbonate (HCO_3^-) electrolytes. Through a rapid equilibrium with the dissolved CO_2, bicarbonate actively participates in eCO_2R under the test conditions. This was further proved in a report by Li et al., in which they directly fed a HCO_3^- solution in the absence of CO_2 gases and generated CO on Ag GDE in a flow cell.[75] More importantly, these studies showed the possibility of an electrochemical reduction of a HCO_3^- solution at an appreciable current density, which has been demonstrated experimentally.

Beyond CO, more predicted reaction intermediates have been successfully observed on SEIRAS. For example, the carboxyl intermediate *COOH was detected on a Ag electrode, which indicates the first step of proton-coupled electron transfer for CO production.[76] By using time-resolved SEIRAS, two distinct intermediates, *CHO and *OCCO, were proved to be involved in two separate pathways toward C_1 (CH_4) and C_2 (C_2H_4) products on Cu, respectively.[77] Furthermore, different metal surfaces showed different affinities for C or O of these intermediates, which can also explain the product selectivity.[78]

Compared to ATR-SEIRAS, surface-enhanced Raman spectroscopy (SERS) could provide additional information on the interactions between metal surfaces and adsorbed species, usually present in low wavenumber ranges (<800 cm^{-1}). Therefore, we applied SERS to investigate the Cu surface under reaction conditions and observed the existence of adsorbed CuO_x and $Cu(OH)_x/O_y$ species even at a lower potential of −0.8 V (Figure 4b).[3] In contrast to the metallic state of Cu surfaces under reduction potentials, as suggested by operando X-ray absorption spectroscopy (XAS),[1] SERS results revealed an "oxygenated" surface of the Cu catalyst, which more likely reflects the true nature of the Cu surface under the reaction conditions due to the higher sensitivity of the SERS technique in comparison to XAS. Despite similar oxygenated species on several nanostructured Cu surfaces, we observed a different selectivity toward C_{2+} products depending on the type of catalyst surface used. Oxide-derived Cu exhibited the highest production rate of oxygenated species among all nanostructured Cu catalysts. Further studies are still needed to elucidate the mechanisms of how the surface oxygenated species are involved in eCO_2R and eCOR.[31,50,79,80] Through subsecond time-resolved SERS, An et al. found that the oxygenates form after several seconds (7 s) upon applying a cathodic potential, which is due to the high surface alkalinity, as the eCO_2R occurs after the redeposition of leached Cu^{2+} in the electrolyte.[81] At the same time, the high surface enhancement of this reconstructed and roughened surface allowed a dynamic monitoring of the evolution of the CO configuration every 0.7 s, which was an improvement of this method.

To complement the surface-enhanced vibrational spectroscopies, techniques that allow us to detect reaction intermediates directly (e.g., oxygenates) are also highly attractive.[82] In a recent study, we developed a flow electrolyzer mass spectrometry (FEMS) device by incorporating a gas-diffusion electrode design in a flow electrochemical reactor, which enables the detection of reactive volatile or gaseous species at high current densities (>100 mA cm^{-2}) (Figure 4c).[51] In ^{18}O labeled water experiments, we found that the oxygen in the as-formed acetaldehyde intermediate was not ^{18}O labeled, suggesting its oxygen originated from the reactant CO. Additionally, most alcohols (i.e., ethanol and *n*-propanol) were ^{18}O labeled. Therefore, their formations are likely through a further reduction of aldehydes after an oxygen exchange process. The unique capability of the FEMS technique will allow us to probe reactive intermediates in other gas-phase electrocatalytic reactions, such as NO_x reduction reactions.[53]

5. TOWARD THE PRACTICAL CO_2 ELECTROLYSIS SYSTEMS

Currently, most research on CO_2 electroreduction has been conducted using a highly pure CO_2 feed; however, the compatibility of CO_2 electroreduction with CO_2 captured from realistic point sources, such as chemical and power plants, has not been scrutinized. CO_2 captured from point sources often contains impurities, such as NO_x, SO_x, O_2, and VOCs (Figure 5).[83,84] Therefore, a comprehensive understanding of these impurities is essential to guide the future deployment of CO_2 electrolysis technologies. In this regard, we studied the impact of SO_2[2] and NO_x[53] on CO_2 electroreduction using Cu, Ag, and Sn catalysts.

On the one hand, the presence of SO_2 induced an FE loss in all three catalysts due to the preferential reduction of SO_2 over CO_2 and formed metal sulfides; however, the eCO_2R performance quickly recovered for Ag and Sn after SO_2 was removed. On the other hand, Cu not only showed a loss in FE but also a dramatic shift in selectivity toward formate and the complete suppression of C_{2+} products. The effect of SO_2 was irreversible on Cu, and formate remained the primary product after SO_2 had been removed from the CO_2 stream. Various characterizations and computational studies suggested that the formation of copper sulfide was responsible for the selectivity shift and that eliminating sulfur species from Cu was extremely difficult. While a trace amount of SO_2 in the CO_2 stream was compatible with Ag and Sn, it was detrimental to Cu.

Turning to NO_x impurities, the presence of NO_x (i.e., NO, NO_2, and N_2O) also reduced the eCO_2R FE, with minimal change in product selectivity, and the performance recovered after NO_x was removed from the CO_2 stream on Ag, Sn, and Cu. N from NO_x incorporated into the carbon support but did not affect the metal catalysts, supporting that NO_x compounds do not affect the catalytic property of the metal catalysts. NO (nitric oxide) was converted to N_2, nitrous oxide (N_2O), ammonia (NH_3), and hydroxylamine (NH_2OH). An investigation of NO's impact at the typical concentrations of NO_x in flue gases revealed that, although NO_x can reduce the efficiency of CO_2 electroreduction, it is compatible.

These studies motivate the demonstration of CO_2 electrolysis using simulated flue gases and the development of impurity-resistant catalysts. Although the production of C_{2+} products is highly desired, it may not be possible to use CO_2 captured from point sources due to the detrimental effect of SO_2 on Cu. Thus, the development of impurity, especially SO_2, resistant C_{2+} formation catalysts may be crucial. Furthermore, CO_2 from a direct air capture may be promising, as these do not contain the above-mentioned impurities. Direct air capture technology has already been implemented in a pilot plant, and the CO_2 capture price is expected to decrease with technology development.[85]

As much progress has been rapidly achieved in eCO_2R technologies, a comprehensive techno-economic analysis is essential to assess the economic feasibility and identify critical challenges and opportunities of eCO_2R technologies.[86−89] Our recent techno-economic analysis was conducted with baseline parameters of electricity price of 0.03 USD kWh^{-1}, stack cost of 550 USD kW^{-1}, MEA replacement period of one year, and the cost of CO_2 of 40 USD tonne-CO_2^{-1}.[4] An analysis suggests that the production costs of C_1 products (e.g., CO and formic acid) are already competitive with conventional processes, with 0.44 and 0.59 USD/kg, respectively. For CO production, electrolyzer parameters were assumed as AEM, 2.6 V, 500 mA cm^{-2}, 30% single-pass conversion, and 95% FE, while for formic acid production, they were assumed as bipolar membrane (BPM), 3.5 V, 200 mA cm^{-2}, 70% single-pass conversion, and 85% FE. Types of membranes were chosen based on the membrane cost analysis.

However, the production of C_{2+} products (i.e., ethylene and ethanol) requires a substantial improvement due to high costs of 2.50 and 2.06 USD/kg, respectively. For ethylene production, electrolyzer parameters were assumed as AEM, 2.9 V, 1000 mA cm^{-2}, 15% single-pass conversion, and 70% FE, while for ethanol production, they were assumed as AEM, 2.5 V, 500 mA cm^{-2}, 15% single-pass conversion, and 60% FE. On the basis of the analysis, the most impactful and vital challenge to make C_{2+} product production economically viable is to improve the CO_2 electrolyzer performance (50% energetic efficiency (EE), >80% FE, and 1000 mA cm^{-2}) and reduce the renewable electricity price (0.01 USD/kWh). Bicarbonate formation also severely hinders the economic feasibility of CO_2 electroreduction, so strategies to mitigate this issue are needed. Additionally, reducing the stack cost (e.g., replacing the expensive iridium anode) and replacement cost (e.g., increasing the stability to five years) and incorporating economic factors, such as the carbon tax credit and selling hydrogen byproduct, can help lower the production cost.[4,7,62]

A two-step eCO_2R process, in which CO_2 is converted to CO in the first CO_2 electrolyzer and CO is further converted to C_{2+} products in the second CO electrolyzer, has been proposed as an effective carbon utilization strategy.[28,54] This strategy benefits from reduced carbonate formation and improved C_{2+} production rate and selectivity. The techno-economic analysis of the two-step conversion process, with optimistic parameters of 90% FE, 50% single-pass conversion, 300 mA cm^{-2}, and 2 V for both eCO_2R and eCOR, revealed that, while the production of ethylene requires a substantial improvement, the production of acetic acid may be immediately profitable. At 2 V, acetic acid and ethylene productions became competitive at electricity prices below 0.05 and 0.033 USD/kWh, respectively. Currently, the state-of-the-art Cu-based catalysts produce a broad mix of products. The development of more selective catalysts can improve the profitability. Furthermore, acetic acid is produced in the form of acetate in alkaline electrolytes, so it requires an additional process to generate acetic acid. Thus, a research effort to produce acetic acid at neutral conditions is desired.[54]

6. CONCLUSION AND OUTLOOK

In this Account, we have summarized our recent contributions in electrocatalyst development, reactor engineering, operando characterizations, and research efforts for practical CO_2 electrolysis systems. Although recent advancements in reactor designs (i.e., vapor-fed electrolyzers) pushed current densities toward industry-applicable levels, technical challenges still need to be addressed before commercialization. Costs associated with an electrolyzer contribute the most to the eCO_2R products costs, so improving the electrolyzer performance (50% EE, >80% FE, and 1000 mA cm^{-2}) remains the most pressing challenge.[4,7] Furthermore, strategies to achieve a higher CO_2 conversion and mitigate the bi/carbonate formation is needed. For instance, a high CO_2 conversion (up to 85%) was demonstrated using acidic electrolytes and various membranes (i.e., cation exchange and bipolar membranes),[12,65,66] though the selectivity and cell potential were worsened. Tandem electrolysis is also promising, employing a low temperature or solid oxide CO_2 electrolyzer to produce CO in the first step, followed by a sequential reduction of CO to C_{2+} products.[28,90] This strategy allows for a more effective C_{2+} product production with a reduced/eliminated bicarbonate/carbonate formation.

Other strategies, such as coupling CO_2/CO electroreduction with other processes or reactants, can potentially enable the production of more valuable chemicals and expand the application of eCO_2R and eCOR.[6] For instance, butanol and hexanol can be produced via an electrocatalytic-biological hybrid process, in which CO_2 is electrochemically converted to synthesis gas (i.e., CO and H_2) followed by biological conversion using bacteria (i.e., *Clostridium autoethanogenum* and *Clostridium kluyveri*).[91] Electrochemically produced synthesis gas can also be upgraded to synthetic fuels using the thermocatalytic Fischer−Tropsch process.[92] As we have demonstrated with the production of amides via the coelectrolysis of CO and amines, new chemicals beyond C_1 and C_2 products can also be produced through a coelectrolysis.[93] The coelectrolysis of CO_2/CO with other reactants remains largely unexplored, and it offers new opportunities for eCO_2R and eCOR.

■ AUTHOR INFORMATION

Corresponding Author

Feng Jiao − *Center for Catalytic Science and Technology, Department of Chemical and Biomolecular Engineering, University of Delaware, Newark, Delaware 19716, United States;* orcid.org/0000-0002-3335-3203; Email: jiao@udel.edu

Authors

Sean Overa − *Center for Catalytic Science and Technology, Department of Chemical and Biomolecular Engineering, University of Delaware, Newark, Delaware 19716, United States*

Byung Hee Ko − *Center for Catalytic Science and Technology, Department of Chemical and Biomolecular Engineering, University of Delaware, Newark, Delaware 19716, United States*

Yaran Zhao − *Center for Catalytic Science and Technology, Department of Chemical and Biomolecular Engineering, University of Delaware, Newark, Delaware 19716, United States*

Complete contact information is available at: https://pubs.acs.org/10.1021/acs.accounts.1c00674

Author Contributions

[†]These authors contributed equally to this work.

Notes

The authors declare no competing financial interest.

Biographies

Sean Overa is a chemical engineering Ph.D. candidate at the University of Delaware, United States, currently working for Prof. Feng Jiao. His research focuses on the conversion of carbon dioxide and carbon monoxide to valuable chemicals. He also works on the scaling of electrochemical reactors.

Byung Hee Ko is a chemical engineering Ph.D. candidate at the University of Delaware, United States, working with Prof. Feng Jiao. His research focuses on the electrochemical conversion of various chemicals, including CO_2, CO, and NO_x.

Yaran Zhao received her doctoral degree in physical chemistry from Nankai University, China, in 2019. She then worked with Prof. Feng Jiao, Prof. Bingjun Xu, and Prof. Levi Thompson as a postdoctoral researcher at the University of Delaware. Her research interests include surface-enhanced Raman spectroscopy and the operando characterization of electrochemical reactions.

Feng Jiao is now the Robert Grasselli Development Professor of Chemical and Biomolecular Engineering and the Director of Center for Catalytic Science & Technology at the University of Delaware. Professor Jiao's group focuses primarily on nanostructured materials, electrocatalysis, and carbon dioxide utilization.

■ ACKNOWLEDGMENTS

The authors acknowledge the financial support from the U.S. Department of Energy, under Award No. DE-FE0031910, and the National Science Foundation (CBET-1904966).

■ REFERENCES

(1) Jouny, M.; Luc, W.; Jiao, F. High-Rate Electroreduction of Carbon Monoxide to Multi-Carbon Products. *Nat. Catal.* **2018**, *1*, 748−755.

(2) Luc, W.; Ko, B. H.; Kattel, S.; Li, S.; Su, D.; Chen, J. G.; Jiao, F. SO_2-Induced Selectivity Change in CO_2 Electroreduction. *J. Am. Chem. Soc.* **2019**, *141*, 9902−9909.

(3) Zhao, Y.; Chang, X.; Malkani, A. S.; Yang, X.; Thompson, L.; Jiao, F.; Xu, B. Speciation of Cu Surfaces during the Electrochemical CO Reduction Reaction. *J. Am. Chem. Soc.* **2020**, *142*, 9735−9743.

(4) Shin, H.; Hansen, K. U.; Jiao, F. Techno-Economic Assessment of Low-Temperature Carbon Dioxide Electrolysis. *Nat. Sustain.* **2021**, *4*, 911−919.

(5) IPCC. *Climate Change 2021: The Physical Science Basis. Contribution of Working Group I to the Sixth Assessment Report of the Intergovernmental Panel on Climate Change;* Masson-Delmotte, V., Zhai, P., Pirani, A., Connors, S.L., Péan, C., Berger, S., Caud, N., Chen, Y., Goldfarb, L., Gomis, M.I., Huang, M., Leitzell, K., Lonnoy, E., Matthews, J.B.R., Maycock, T.K., Waterfield, T., Yelekçi, O., Yu, R., Zhou, B., Eds.; Cambridge University Press. In Press.

(6) Overa, S.; Feric, T. G.; Park, A. H. A.; Jiao, F. Tandem and Hybrid Processes for Carbon Dioxide Utilization. *Joule* **2021**, *5*, 8−13.

(7) Jouny, M.; Luc, W.; Jiao, F. General Techno-Economic Analysis of CO_2 Electrolysis Systems. *Ind. Eng. Chem. Res.* **2018**, *57*, 2165−2177.

(8) Cho, M. K.; Park, H. Y.; Lee, H. J.; Kim, H. J.; Lim, A.; Henkensmeier, D.; Yoo, S. J.; Kim, J. Y.; Lee, S. Y.; Park, H. S.; Jang, J. H. Alkaline Anion Exchange Membrane Water Electrolysis: Effects of Electrolyte Feed Method and Electrode Binder Content. *J. Power Sources* **2018**, *382*, 22−29.

(9) Luo, T.; Abdu, S.; Wessling, M. Selectivity of Ion Exchange Membranes: A Review. *J. Membr. Sci.* **2018**, *555*, 429−454.

(10) Lv, J. J.; Jouny, M.; Luc, W.; Zhu, W.; Zhu, J. J.; Jiao, F. A Highly Porous Copper Electrocatalyst for Carbon Dioxide Reduction. *Adv. Mater.* **2018**, *30*, 1−8.

(11) Verma, S.; Hamasaki, Y.; Kim, C.; Huang, W.; Lu, S.; Jhong, H. R. M.; Gewirth, A. A.; Fujigaya, T.; Nakashima, N.; Kenis, P. J. A. Insights into the Low Overpotential Electroreduction of CO_2 to CO on a Supported Gold Catalyst in an Alkaline Flow Electrolyzer. *ACS Energy Lett.* **2018**, *3*, 193−198.

(12) Huang, J. E.; Li, F.; Ozden, A.; Sedighian Rasouli, A.; Garcia de Arquer, F. P.; Liu, S.; Zhang, S.; Luo, M.; Wang, X.; Lum, Y.; Xu, Y.; Bertens, K.; Miao, R. K.; Dinh, C.-T.; Sinton, D.; Sargent, E. H. CO_2 Electrolysis to Multicarbon Products in Strong Acid. *Science* **2021**, *372*, 1074−1078.

(13) Wang, Z. L.; Choi, J.; Xu, M.; Hao, X.; Zhang, H.; Jiang, Z.; Zuo, M.; Kim, J.; Zhou, W.; Meng, X.; Yu, Q.; Sun, Z.; Wei, S.; Ye, J.; Wallace, G. G.; Officer, D. L.; Yamauchi, Y. Optimizing Electron Densities of Ni-N-C Complexes by Hybrid Coordination for Efficient Electrocatalytic CO_2 Reduction. *ChemSusChem* **2020**, *13*, 929−937.

(14) Zhao, Y.; Zheng, L.; Jiang, D.; Xia, W.; Xu, X.; Yamauchi, Y.; Ge, J.; Tang, J. Nanoengineering Metal-Organic Framework-Based Materials for Use in Electrochemical CO_2 Reduction Reactions. *Small* **2021**, *17*, 2006590.

(15) Han, N.; Wang, Y.; Yang, H.; Deng, J.; Wu, J.; Li, Y.; Li, Y. Ultrathin Bismuth Nanosheets from in Situ Topotactic Transformation for Selective Electrocatalytic CO_2 Reduction to Formate. *Nat. Commun.* **2018**, *9*, 1320.

(16) Gong, Q.; Ding, P.; Xu, M.; Zhu, X.; Wang, M.; Deng, J.; Ma, Q.; Han, N.; Zhu, Y.; Lu, J.; Feng, Z.; Li, Y.; Zhou, W.; Li, Y. Structural Defects on Converted Bismuth Oxide Nanotubes Enable Highly Active Electrocatalysis of Carbon Dioxide Reduction. *Nat. Commun.* **2019**, *10*, 2807.

(17) Yang, F.; Song, P.; Liu, X.; Mei, B.; Xing, W.; Jiang, Z.; Gu, L.; Xu, W. Highly Efficient CO_2 Electroreduction on ZnN_4-Based Single-Atom Catalyst. *Angew. Chemie - Int. Ed.* **2018**, *57*, 12303−12307.

(18) Won, D. H.; Shin, H.; Koh, J.; Chung, J.; Lee, H. S.; Kim, H.; Woo, S. I. Highly Efficient, Selective, and Stable CO_2 Electroreduction on a Hexagonal Zn Catalyst. *Angew. Chemie - Int. Ed.* **2016**, *55*, 9297−9300.

(19) Ma, W.; Xie, S.; Liu, T.; Fan, Q.; Ye, J.; Sun, F.; Jiang, Z.; Zhang, Q.; Cheng, J.; Wang, Y. Electrocatalytic Reduction of CO_2 to Ethylene and Ethanol through Hydrogen-Assisted C-C Coupling over Fluorine-Modified Copper. *Nat. Catal.* **2020**, *3*, 478−487.

(20) García de Arquer, F. P.; Dinh, C. T.; Ozden, A.; Wicks, J.; McCallum, C.; Kirmani, A. R.; Nam, D. H.; Gabardo, C.; Seifitokaldani, A.; Wang, X.; Li, Y. C.; Li, F.; Edwards, J.; Richter, L. J.; Thorpe, S. J.; Sinton, D.; Sargent, E. H. CO_2 Electrolysis to Multicarbon Products at Activities Greater than 1 A cm^{-2}. *Science.* **2020**, *367*, 661−666.

(21) Yang, H.; Kaczur, J. J.; Sajjad, S. D.; Masel, R. I. Performance and Long-Term Stability of CO_2 conversion to Formic Acid Using a Three-Compartment Electrolyzer Design. *J. CO_2 Util.* **2020**, *42*, 101349.

(22) Theaker, N.; Strain, J. M.; Kumar, B.; Brian, J. P.; Kumari, S.; Spurgeon, J. M. Heterogeneously Catalyzed Two-Step Cascade Electrochemical Reduction of CO_2 to Ethanol. *Electrochim. Acta* **2018**, *274*, 1−8.

(23) Liu, Z.; Yang, H.; Kutz, R.; Masel, R. I. CO_2 Electrolysis to CO and O_2 at High Selectivity, Stability and Efficiency Using Sustainion Membranes. *J. Electrochem. Soc.* **2018**, *165*, J3371−J3377.

(24) Bushuyev, O. S.; De Luna, P.; Dinh, C. T.; Tao, L.; Saur, G.; van de Lagemaat, J.; Kelley, S. O.; Sargent, E. H. What Should We Make with CO_2 and How Can We Make It? *Joule* **2018**, *2*, 825−832.

(25) Li, F.; Li, Y. C.; Wang, Z.; Li, J.; Nam, D. H.; Lum, Y.; Luo, M.; Wang, X.; Ozden, A.; Hung, S. F.; Chen, B.; Wang, Y.; Wicks, J.; Xu, Y.; Li, Y.; Gabardo, C. M.; Dinh, C. T.; Wang, Y.; Zhuang, T.; Sinton, D.; Sargent, E. H. Cooperative CO_2-to-Ethanol Conversion via Enriched Intermediates at Molecule-Metal Catalyst Interfaces. *Nat. Catal.* **2020**, *3*, 75−82.

(26) Dinh, C. T.; Burdyny, T.; Kibria, G.; Seifitokaldani, A.; Gabardo, C. M.; García De Arquer, F. P.; Kiani, A.; Edwards, J. P.; De Luna, P.; Bushuyev, O. S.; Zou, C.; Quintero-Bermudez, R.; Pang, Y.; Sinton, D.; Sargent, E. H. CO_2 Electroreduction to Ethylene via Hydroxide-Mediated Copper Catalysis at an Abrupt Interface. *Science* **2018**, *360*, 783−787.

(27) Yang, H.; Kaczur, J. J.; Sajjad, S. D.; Masel, R. I. Electrochemical Conversion of CO_2 to Formic Acid Utilizing Sustainion^{TM} Membranes. *J. CO_2 Util.* **2017**, *20*, 208−217.

(28) Ozden, A.; Wang, Y.; Li, F.; Luo, M.; Sisler, J.; Thevenon, A.; Rosas-Hernández, A.; Burdyny, T.; Lum, Y.; Yadegari, H.; Agapie, T.; Peters, J. C.; Sargent, E. H.; Sinton, D. Cascade CO_2 Electroreduction Enables Efficient Carbonate-Free Production of Ethylene. *Joule* **2021**, *5*, 706−719.

(29) Lu, Q.; Rosen, J.; Jiao, F. Nanostructured Metallic Electrocatalysts for Carbon Dioxide Reduction. *ChemCatChem.* **2015**, *7*, 38−47.

(30) Kortlever, R.; Shen, J.; Schouten, K. J. P.; Calle-Vallejo, F.; Koper, M. T. M. Catalysts and Reaction Pathways for the Electrochemical Reduction of Carbon Dioxide. *J. Phys. Chem. Lett.* **2015**, *6*, 4073−4082.

(31) Mistry, H.; Varela, A. S.; Bonifacio, C. S.; Zegkinoglou, I.; Sinev, I.; Choi, Y. W.; Kisslinger, K.; Stach, E. A.; Yang, J. C.; Strasser, P.; Cuenya, B. R. Highly Selective Plasma-Activated Copper Catalysts for Carbon Dioxide Reduction to Ethylene. *Nat. Commun.* **2016**, *7*, 12123.

(32) Wang, Z. L.; Li, C.; Yamauchi, Y. Nanostructured Nonprecious Metal Catalysts for Electrochemical Reduction of Carbon Dioxide. *Nano Today* **2016**, *11*, 373−391.

(33) Lu, Q.; Rosen, J.; Zhou, Y.; Hutchings, G. S.; Kimmel, Y. C.; Chen, J. G.; Jiao, F. A Selective and Efficient Electrocatalyst for Carbon Dioxide Reduction. *Nat. Commun.* **2014**, *5*, 3242.

(34) Rosen, J.; Hutchings, G. S.; Lu, Q.; Forest, R. V.; Moore, A.; Jiao, F. Electrodeposited Zn Dendrites with Enhanced CO Selectivity for Electrocatalytic CO_2 Reduction. *ACS Catal.* **2015**, *5*, 4586−4591.

(35) Chen, A.; Zhang, X.; Chen, L.; Yao, S.; Zhou, Z. A Machine Learning Model on Simple Features for CO_2 Reduction Electrocatalysts. *J. Phys. Chem. C* **2020**, *124*, 22471−22478.

(36) Nitopi, S.; Bertheussen, E.; Scott, S. B.; Liu, X.; Engstfeld, A. K.; Horch, S.; Seger, B.; Stephens, I. E. L.; Chan, K.; Hahn, C.; Nørskov, J. K.; Jaramillo, T. F.; Chorkendorff, I. Progress and Perspectives of Electrochemical CO_2 Reduction on Copper in Aqueous Electrolyte. *Chem. Rev.* **2019**, *119*, 7610−7672.

(37) Endrődi, B.; Kecsenovity, E.; Samu, A.; Darvas, F.; Jones, R. V.; Török, V.; Danyi, A.; Janáky, C. Multilayer Electrolyzer Stack Converts Carbon Dioxide to Gas Products at High Pressure with High Efficiency. *ACS Energy Lett.* **2019**, *4*, 1770−1777.

(38) Jeng, E.; Jiao, F. Investigation of CO_2 single-Pass Conversion in a Flow Electrolyzer. *React. Chem. Eng.* **2020**, *5*, 1768−1775.

(39) Hori, Y.; Wakebe, H.; Tsukamoto, T.; Koga, O. Electrocatalytic Process of CO Selectivity in Electrochemical Reduction of CO_2 at Metal Electrodes in Aqueous Media. *Electrochim. Acta* **1994**, *39*, 1833−1839.

(40) Salehi-Khojin, A.; Jhong, H. R. M.; Rosen, B. A.; Zhu, W.; Ma, S.; Kenis, P. J. A.; Masel, R. I. Nanoparticle Silver Catalysts That Show Enhanced Activity for Carbon Dioxide Electrolysis. *J. Phys. Chem. C* **2013**, *117*, 1627−1632.

(41) Back, S.; Yeom, M. S.; Jung, Y. Active Sites of Au and Ag Nanoparticle Catalysts for CO_2 Electroreduction to CO. *ACS Catal.* **2015**, *5*, 5089−5096.

(42) Yang, C.; Ko, B. H.; Hwang, S.; Liu, Z.; Yao, Y.; Luc, W.; Cui, M.; Malkani, A. S.; Li, T.; Wang, X.; Dai, J.; Xu, B.; Wang, G.; Su, D.; Jiao, F.; Hu, L. Overcoming Immiscibility toward Bimetallic Catalyst Library. *Sci. Adv.* **2020**, *6*, No. eaaz6844.

(43) Zhong, M.; Tran, K.; Min, Y.; Wang, C.; Wang, Z.; Dinh, C. T.; De Luna, P.; Yu, Z.; Rasouli, A. S.; Brodersen, P.; Sun, S.; Voznyy, O.; Tan, C.; Askerka, M.; Che, F.; Liu, M.; Seifitokaldani, A.; Pang, Y.; Lo, S.; Ip, A.; Ulissi, Z.; Sargent, E. H. Accelerated Discovery of CO_2 Electrocatalysts Using Active Machine Learning. *Nature* **2020**, *581*, 178−183.

(44) Liu, X.; Xiao, J.; Peng, H.; Hong, X.; Chan, K.; Nørskov, J. K. Understanding Trends in Electrochemical Carbon Dioxide Reduction Rates. *Nat. Commun.* **2017**, *8*, 15438.

(45) Sankar, M.; Dimitratos, N.; Miedziak, P. J.; Wells, P. P.; Kiely, C. J.; Hutchings, G. J. Designing Bimetallic Catalysts for a Green and Sustainable Future. *Chem. Soc. Rev.* **2012**, *41*, 8099−8139.

(46) Wang, D.; Li, Y. Bimetallic Nanocrystals: Liquid-Phase Synthesis and Catalytic Applications. *Adv. Mater.* **2011**, *23*, 1044−1060.

(47) Gilroy, K. D.; Ruditskiy, A.; Peng, H. C.; Qin, D.; Xia, Y. Bimetallic Nanocrystals: Syntheses, Properties, and Applications. *Chem. Rev.* **2016**, *116*, 10414−10472.

(48) Yao, Y.; Huang, Z.; Hughes, L. A.; Gao, J.; Li, T.; Morris, D.; Zeltmann, S. E.; Savitzky, B. H.; Ophus, C.; Finfrock, Y. Z.; Dong, Q.; Jiao, M.; Mao, Y.; Chi, M.; Zhang, P.; Li, J.; Minor, A. M.; Shahbazian-Yassar, R.; Hu, L. Extreme Mixing in Nanoscale Transition Metal Alloys. *Matter* **2021**, *4*, 2340−2353.

(49) Whipple, D. T.; Finke, E. C.; Kenis, P. J. A. Microfluidic Reactor for the Electrochemical Reduction of Carbon Dioxide: The Effect of PH. *Electrochem. Solid-State Lett.* **2010**, *13*, B109.

(50) Li, C. W.; Ciston, J.; Kanan, M. W. Electroreduction of Carbon Monoxide to Liquid Fuel on Oxide-Derived Nanocrystalline Copper. *Nature* **2014**, *508*, 504−507.

(51) Hasa, B.; Jouny, M.; Ko, B. H.; Xu, B.; Jiao, F. Flow Electrolyzer Mass Spectrometry with a Gas-Diffusion Electrode Design. *Angew. Chemie - Int. Ed.* **2021**, *60*, 3277−3282.

(52) Luc, W.; Fu, X.; Shi, J.; Lv, J. J.; Jouny, M.; Ko, B. H.; Xu, Y.; Tu, Q.; Hu, X.; Wu, J.; Yue, Q.; Liu, Y.; Jiao, F.; Kang, Y. Two-Dimensional Copper Nanosheets for Electrochemical Reduction of Carbon Monoxide to Acetate. *Nat. Catal.* **2019**, *2*, 423−430.

(53) Ko, B. H.; Hasa, B.; Shin, H.; Jeng, E.; Overa, S.; Chen, W.; Jiao, F. The Impact of Nitrogen Oxides on Electrochemical Carbon Dioxide Reduction. *Nat. Commun.* **2020**, *11*, 5856.

(54) Jouny, M.; Hutchings, G. S.; Jiao, F. Carbon Monoxide Electroreduction as an Emerging Platform for Carbon Utilization. *Nat. Catal.* **2019**, *2*, 1062−1070.

(55) Xing, Z.; Hu, L.; Ripatti, D. S.; Hu, X.; Feng, X. Enhancing Carbon Dioxide Gas-Diffusion Electrolysis by Creating a Hydrophobic Catalyst Microenvironment. *Nat. Commun.* **2021**, *12*, 136.

(56) Nguyen, T. N.; Dinh, C. T. Gas Diffusion Electrode Design for Electrochemical Carbon Dioxide Reduction. *Chem. Soc. Rev.* **2020**, *49*, 7488−7504.

(57) Yin, Z.; Peng, H.; Wei, X.; Zhou, H.; Gong, J.; Huai, M.; Xiao, L.; Wang, G.; Lu, J.; Zhuang, L. An Alkaline Polymer Electrolyte CO_2 Electrolyzer Operated with Pure Water. *Energy Environ. Sci.* **2019**, *12*, 2455.

(58) Ripatti, D. S.; Veltman, T. R.; Kanan, M. W. Carbon Monoxide Gas Diffusion Electrolysis That Produces Concentrated C_2 Products with High Single-Pass Conversion. *Joule* **2019**, *3*, 240−256.

(59) Miller, M.; Bazylak, A. A Review of Polymer Electrolyte Membrane Fuel Cell Stack Testing. *J. Power Sources* **2011**, *196*, 601−613.

(60) Tawfik, H.; Hung, Y.; Mahajan, D. Metal Bipolar Plates for PEM Fuel Cell-A Review. *J. Power Sources* **2007**, *163*, 755−767.

(61) Manso, A. P.; Marzo, F. F.; Barranco, J.; Garikano, X.; Garmendia Mujika, M. Influence of Geometric Parameters of the Flow Fields on the Performance of a PEM Fuel Cell. A Review. *Int. J. Hydrogen Energy* **2012**, *37*, 15256−15287.

(62) Rabinowitz, J. A.; Kanan, M. W. The Future of Low-Temperature Carbon Dioxide Electrolysis Depends on Solving One Basic Problem. *Nat. Commun.* **2020**, *11*, 5231.

(63) Salvatore, D. A.; Weekes, D. M.; He, J.; Dettelbach, K. E.; Li, Y. C.; Mallouk, T. E.; Berlinguette, C. P. Electrolysis of Gaseous CO_2 to CO in a Flow Cell with a Bipolar Membrane. *ACS Energy Lett.* **2018**, *3*, 149−154.

(64) Vermaas, D. A.; Smith, W. A. Synergistic Electrochemical CO2 Reduction and Water Oxidation with a Bipolar Membrane. *ACS Energy Lett.* **2016**, *1*, 1143−1148.

(65) Yan, Z.; Hitt, J. L.; Zeng, Z.; Hickner, M. A.; Mallouk, T. E. Improving the Efficiency of CO_2 Electrolysis by Using a Bipolar Membrane with a Weak-Acid Cation Exchange Layer. *Nat. Chem.* **2021**, *13*, 33−40.

(66) O'Brien, C. P.; Miao, R. K.; Liu, S.; Xu, Y.; Lee, G.; Robb, A.; Huang, J. E.; Xie, K.; Bertens, K.; Gabardo, C. M.; Edwards, J. P.; Dinh, C. T.; Sargent, E. H.; Sinton, D. Single Pass CO_2 Conversion Exceeding 85% in the Electrosynthesis of Multicarbon Products via Local CO_2 Regeneration. *ACS Energy Lett.* **2021**, *6*, 2952−2959.

(67) Mittal, C.; Hadsbjerg, C.; Blennow, P. Small-Scale CO from CO_2 Using Electrolysis. *Chem. Eng. World* **2017**, *52*, 44−46.

(68) Zhang, L.; Hu, S.; Zhu, X.; Yang, W. Electrochemical Reduction of CO_2 in Solid Oxide Electrolysis Cells. *J. Energy Chem.* **2017**, *26*, 593−601.

(69) Küngas, R.; Blennow, P.; Heiredal-Clausen, T.; Holt, T.; Rass-Hansen, J.; Primdahl, S.; Hansen, J. B. ECOs - A Commercial CO_2 Electrolysis System Developed by Haldor Topsoe. *ECS Trans.* **2017**, *78*, 2879−2884.

(70) Gunathunge, C. M.; Li, X.; Li, J.; Hicks, R. P.; Ovalle, V. J.; Waegele, M. M. Spectroscopic Observation of Reversible Surface Reconstruction of Copper Electrodes under CO2 Reduction. *J. Phys. Chem. C* **2017**, *121*, 12337−12344.

(71) Gunathunge, C. M.; Ovalle, V. J.; Li, Y.; Janik, M. J.; Waegele, M. M. Existence of an Electrochemically Inert CO Population on Cu Electrodes in Alkaline PH. *ACS Catal.* **2018**, *8*, 7507−7516.

(72) Malkani, A. S.; Li, J.; Oliveira, N. J.; He, M.; Chang, X.; Xu, B.; Lu, Q. Understanding the Electric and Nonelectric Field Components of the Cation Effect on the Electrochemical CO Reduction Reaction. *Sci. Adv.* **2020**, *6*, No. eabd2569.

(73) Malkani, A. S.; Anibal, J.; Chang, X.; Xu, B. Bridging the Gap in the Mechanistic Understanding of Electrocatalysis via In Situ Characterizations. *iScience* **2020**, *23*, 101776.

(74) Dunwell, M.; Lu, Q.; Heyes, J. M.; Rosen, J.; Chen, J. G.; Yan, Y.; Jiao, F.; Xu, B. The Central Role of Bicarbonate in the Electrochemical Reduction of Carbon Dioxide on Gold. *J. Am. Chem. Soc.* **2017**, *139*, 3774−3783.

(75) Li, T.; Lees, E. W.; Goldman, M.; Salvatore, D. A.; Weekes, D. M.; Berlinguette, C. P. Electrolytic Conversion of Bicarbonate into CO in a Flow Cell. *Joule* **2019**, *3*, 1487−1497.

(76) Firet, N. J.; Smith, W. A. Probing the Reaction Mechanism of CO_2 Electroreduction over Ag Films via Operando Infrared Spectroscopy. *ACS Catal.* **2017**, *7*, 606−612.

(77) Kim, Y.; Park, S.; Shin, S. J.; Choi, W.; Min, B. K.; Kim, H.; Kim, W.; Hwang, Y. J. Time-Resolved Observation of C-C Coupling Intermediates on Cu Electrodes for Selective Electrochemical CO_2 reduction. *Energy Environ. Sci.* **2020**, *13*, 4301−4311.

(78) Katayama, Y.; Nattino, F.; Giordano, L.; Hwang, J.; Rao, R. R.; Andreussi, O.; Marzari, N.; Shao-Horn, Y. An in Situ Surface-Enhanced Infrared Absorption Spectroscopy Study of Electrochemical CO_2 Reduction: Selectivity Dependence on Surface C-Bound and O-Bound Reaction Intermediates. *J. Phys. Chem. C* **2019**, *123*, 5951−5963.

(79) Handoko, A. D.; Ong, C. W.; Huang, Y.; Lee, Z. G.; Lin, L.; Panetti, G. B.; Yeo, B. S. Mechanistic Insights into the Selective Electroreduction of Carbon Dioxide to Ethylene on Cu_2O-Derived Copper Catalysts. *J. Phys. Chem. C* **2016**, *120*, 20058−20067.

(80) Eilert, A.; Cavalca, F.; Roberts, F. S.; Osterwalder, J.; Liu, C.; Favaro, M.; Crumlin, E. J.; Ogasawara, H.; Friebel, D.; Pettersson, L. G. M.; Nilsson, A. Subsurface Oxygen in Oxide-Derived Copper

Electrocatalysts for Carbon Dioxide Reduction. *J. Phys. Chem. Lett.* **2017**, *8*, 285−290.

(81) An, H.; Wu, L.; Mandemaker, L. D. B.; Yang, S.; Ruiter, J.; Wijten, J. H. J.; Janssens, J. C. L.; Hartman, T.; Stam, W.; Weckhuysen, B. M. Sub-Second Time-Resolved Surface-Enhanced Raman Spectroscopy Reveals Dynamic CO Intermediates during Electrochemical CO_2 Reduction on Copper. *Angew. Chemie - Int. Ed.* **2021**, *60*, 16576−16584.

(82) Clark, E. L.; Bell, A. T. Direct Observation of the Local Reaction Environment during the Electrochemical Reduction of CO_2. *J. Am. Chem. Soc.* **2018**, *140*, 7012−7020.

(83) Koytsoumpa, E. I.; Bergins, C.; Kakaras, E. The CO_2 Economy: Review of CO_2 Capture and Reuse Technologies. *J. Supercrit. Fluids* **2018**, *132*, 3−16.

(84) Last, G. V.; Schmick, M. T. *Identification and Selection of Major Carbon Dioxide Stream Compositions;* Pacific Northwest National Laboratory: Richland, WA, 2011.

(85) Fasihi, M.; Efimova, O.; Breyer, C. Techno-Economic Assessment of CO_2 Direct Air Capture Plants. *J. Clean. Prod.* **2019**, *224*, 957−980.

(86) Alerte, T.; Edwards, J. P.; Gabardo, C. M.; O'Brien, C. P.; Gaona, A.; Wicks, J.; Obradović, A.; Sarkar, A.; Jaffer, S. A.; MacLean, H. L.; Sinton, D.; Sargent, E. H. Downstream of the CO_2 Electrolyzer: Assessing the Energy Intensity of Product Separation. *ACS Energy Lett.* **2021**, *6*, 4405−4412.

(87) Somoza-Tornos, A.; Guerra, O. J.; Crow, A. M.; Smith, W. A.; Hodge, B. M. Process Modeling, Techno-Economic Assessment, and Life Cycle Assessment of the Electrochemical Reduction of CO_2: A Review. *iScience* **2021**, *24*, 102813.

(88) Sisler, J.; Khan, S.; Ip, A. H.; Schreiber, M. W.; Jaffer, S. A.; Bobicki, E. R.; Dinh, C. T.; Sargent, E. H. Ethylene Electrosynthesis: A Comparative Techno-Economic Analysis of Alkaline vs Membrane Electrode Assembly vs CO_2-CO-C_2H_4 Tandems. *ACS Energy Lett.* **2021**, *6*, 997−1002.

(89) Prajapati, A.; Singh, M. R. Assessment of Artificial Photosynthetic Systems for Integrated Carbon Capture and Conversion. *ACS Sustain. Chem. Eng.* **2019**, *7*, 5993−6003.

(90) Cuellar, N. S. R.; Scherer, C.; Kackar, B.; Eisenreich, W.; Huber, C.; Wiesner-Fleischer, K.; Fleischer, M.; Hinrichsen, O. Two-Step Electrochemical Reduction of CO_2 towards Multi-Carbon Products at High Current Densities. *J. CO_2 Util.* **2019**, *36*, 263−275.

(91) Haas, T.; Krause, R.; Weber, R.; Demler, M.; Schmid, G. Technical Photosynthesis Involving CO_2 Electrolysis and Fermentation. *Nat. Catal.* **2018**, *1*, 32−39.

(92) Xu, H.; Maroto-Valer, M. M.; Ni, M.; Cao, J.; Xuan, J. Low Carbon Fuel Production from Combined Solid Oxide CO_2 Co-Electrolysis and Fischer−Tropsch Synthesis System: A Modelling Study. *Appl. Energy* **2019**, *242*, 911−918.

(93) Jouny, M.; Lv, J. J.; Cheng, T.; Ko, B. H.; Zhu, J. J.; Goddard, W. A.; Jiao, F. Formation of Carbon-Nitrogen Bonds in Carbon Monoxide Electrolysis. *Nat. Chem.* **2019**, *11*, 846−851.